



Influence of Bi on morphology and optical properties of InAs QDs

Downloaded from: <https://research.chalmers.se>, 2025-12-05 00:14 UTC

Citation for the original published paper (version of record):

Wang, L., Pan, W., Chen, X. et al (2017). Influence of Bi on morphology and optical properties of InAs QDs. Optical Materials Express, 7(12): 4249-4257. <http://dx.doi.org/10.1364/OME.7.004249>

N.B. When citing this work, cite the original published paper.



Influence of Bi on morphology and optical properties of InAs QDs

LIJUAN WANG,^{1,2} WENWU PAN,¹ XIREN CHEN,³ XIAOYAN WU,¹ JUN SHAO,³
AND SHUMIN WANG^{1,4,*}

¹Shanghai Institute of Microsystem and Information Technology, Chinese Academy of Sciences, 865 Chang Ning Road, Shanghai 200050, China

²University of Chinese Academy of Sciences, Beijing 100049, China

³Shanghai Institute of Technical Physics, Chinese Academy of Sciences, 500 Yu Tian Road, Shanghai 200083, China

⁴Department of Microtechnology and Nanoscience, Chalmers University of Technology, Gothenburg 41296, Sweden

*shumin@mail.sim.ac.cn

Abstract: We study the surface morphology and photoluminescence (PL) property of InAs quantum dots (QDs) on GaAs using bismuth (Bi) in the layer prior to or after the growth of QDs. Incorporating Bi in the layer prior to the QD deposition delays the onset of InAs QD formation resulting in a decrease in QD height and density. As a surfactant, adding Bi in the GaAs capping layer at a high growth temperature reduces the In surface diffusion length leading to uniform and well preserved InAs QDs in terms of height and density. The incorporation of 3% Bi at a low growth temperature, which forms a GaAsBi capping layer, can effectively lower the PL transition energy up to 163 meV and reduce the PL linewidth, leading to an emission wavelength of 1.365 μm at 77 K.

© 2017 Optical Society of America

OCIS codes: (020.0020) Atomic and molecular physics; (270.0270) Quantum optics; (300.6210) Spectroscopy, atomic; (300.6280) Spectroscopy, fluorescence and luminescence.

References and links

1. H. Liu, T. Wang, Q. Jiang, R. Hogg, F. Tutu, F. Pozzi, and A. Seeds, "Long-wavelength InAs/GaAs quantum-dot laser diode monolithically grown on Ge substrate," *Nat. Photonics* **5**, 416–419 (2011).
2. S. Wolde, Y.-F. Lao, A. G. Unil Perera, Y. H. Zhang, T. M. Wang, J. O. Kim, T. Schuler-Sandy, Z.-B. Tian, and S. Krishna, "Noise, gain, and capture probability of p-type InAs-GaAs quantum-dot and quantum dot-in-well infrared photodetectors," *J. Appl. Phys.* **121**, 244501 (2017).
3. D. Guimard, R. Morihara, D. Bordel, K. Tanabe, Y. Wakayama, M. Nishioka, and Y. Arakawa, "Fabrication of InAs/GaAs quantum dot solar cells with enhanced photocurrent and without degradation of open circuit voltage," *Appl. Phys. Lett.* **96**, 203507 (2010).
4. Y. H. Jhang, R. Mochida, K. Tanabe, K. Takemasa, M. Sugawara, S. Iwamoto, and Y. Arakawa, "Direct modulation of 1.3 μm quantum dot lasers on silicon at 60 °C," *Opt. Express* **24**(16), 18428–18435 (2016).
5. F. Ferdos, S. Wang, Y. Wei, A. Larsson, M. Sadeghi, and Q. Zhao, "Influence of a thin GaAs cap layer on structural and optical properties of InAs quantum dots," *Appl. Phys. Lett.* **81**, 1195–1197 (2002).
6. N. Ledentsov, A. Kovsh, A. Zhukov, N. Maleev, S. Mikhlin, A. Vasil'ev, E. Semenova, M. Maximov, Y. M. Shernyakov, and N. Kryzhanovskaya, "High performance quantum dot lasers on GaAs substrates operating in 1.5 μm range," *Electron. Lett.* **39**, 1126–1128 (2003).
7. R. Wang, A. Stintz, P. Varangis, T. Newell, H. Li, K. Malloy, and L. Lester, "Room-temperature operation of InAs quantum-dash lasers on InP [001]," *Ieee Photonic Tech L* **13**, 767–769 (2001).
8. N. Nuntawong, S. Birudavolu, C. P. Hains, S. Huang, H. Xu, and D. L. Huffaker, "Effect of strain-compensation in stacked 1.3 μm InAs/GaAs quantum dot active regions grown by metalorganic chemical vapor deposition," *Appl. Phys. Lett.* **85**, 3050–3052 (2004).
9. H. Y. Liu, I. R. Sellers, M. Gutiérrez, K. M. Groom, R. Beanland, W. M. Soong, M. Hopkinson, J. P. R. David, T. J. Badcock, D. J. Mowbray, and M. S. Skolnick, "Optimizing the growth of 1.3- μm InAs/InGaAs dots-in-a-well structure: Achievement of high-performance laser," *Mater. Sci. Eng. C* **25**, 779–783 (2005).
10. M. Usman, D. Vasilev, G. Klimeck, M. I. Caldas, and N. Studart, "Strain-engineered self-organized InAs/GaAs quantum dots for long wavelength (1.3 μm –1.5 μm) optical applications," *AIP Conf. Proc.* **2010**, 527–528 (2010).
11. S. Francoeur, M. J. Seong, A. Mascarenhas, S. Tixier, M. Adamczyk, and T. Tiedje, "Band gap of GaAs_{1-x}Bix, 0<x<3.6%," *Appl. Phys. Lett.* **82**, 3874–3876 (2003).

12. K. Oe, "Characteristics of Semiconductor Alloy GaAs_{1-x}Bi_x," Jpn. J. Appl. Phys. **41**, 2801–2806 (2002).
13. B. Fluegel, S. Francoeur, A. Mascarenhas, S. Tixier, E. C. Young, and T. Tiedje, "Giant spin-orbit bowing in GaAs_{1-x}Bi_x," Phys. Rev. Lett. **97**(6), 067205 (2006).
14. L. Wang, L. Zhang, L. Yue, D. Liang, X. Chen, Y. Li, P. Lu, J. Shao, and S. Wang, "Novel Dilute Bismide, Epitaxy, Physical Properties and Device Application," Crystals **7**, 63 (2017).
15. B. Zvonkov, I. Karpovich, N. Baidus, D. Filatov, S. Morozov, and Y. Y. Gushina, "Surfactant effect of bismuth in the MOVPE growth of the InAs quantum dots on GaAs," Nanotechnology **11**, 221 (2000).
16. V. D. Dasika, E. M. Krivoy, H. P. Nair, S. J. Maddox, K. W. Park, D. Jung, M. L. Lee, E. T. Yu, and S. R. Bank, "Increased InAs quantum dot size and density using bismuth as a surfactant," Appl. Phys. Lett. **105**, 253104 (2014).
17. H. Okamoto, T. Tawara, H. Gotoh, H. Kamada, and T. Sogawa, "Growth and Characterization of Telecommunication-Wavelength Quantum Dots Using Bi as a Surfactant," Jpn. J. Appl. Phys. **49**, 06GJ01 (2010).
18. D. Fan, Z. Zeng, V. G. Dorogan, Y. Hirono, C. Li, Y. I. Mazur, S.-Q. Yu, S. R. Johnson, Z. M. Wang, and G. J. Salamo, "Bismuth surfactant mediated growth of InAs quantum dots by molecular beam epitaxy," J. Mater. Sci. Mater. Electron. **24**, 1635–1639 (2012).
19. P. Wang, W. Pan, X. Wu, J. Liu, C. Cao, S. Wang, and Q. Gong, "Influence of GaAsBi Matrix on Optical and Structural Properties of InAs Quantum Dots," Nanoscale Res. Lett. **11**(1), 280 (2016).
20. Y. Q. Wei, S. M. Wang, F. Ferdos, J. Vukusic, A. Larsson, Q. X. Zhao, and M. Sadeghi, "Large ground-to-first-excited-state transition energy separation for InAs quantum dots emitting at 1.3 μm ," Appl. Phys. Lett. **81**, 1621–1623 (2002).
21. H. Y. Liu, X. D. Wang, J. Wu, B. Xu, Y. Q. Wei, W. H. Jiang, D. Ding, X. L. Ye, F. Lin, J. F. Zhang, J. B. Liang, and Z. G. Wang, "Structural and optical properties of self-assembled InAs/GaAs quantum dots covered by In_xGa_{1-x}As (0 $\leq x \leq 0.3$)," J. Appl. Phys. **88**, 3392–3395 (2000).
22. K. Muraki, S. Fukatsu, Y. Shiraki, and R. Ito, "Surface segregation of In atoms during molecular beam epitaxy and its influence on the energy levels in InGaAs/GaAs quantum wells," Appl. Phys. Lett. **61**, 557–559 (1992).
23. S. M. Wang, T. G. Andersson, and M. J. Ekenstedt, "Interface morphology in molecular beam epitaxy grown In_{0.5}Ga_{0.5}As/GaAs strained heterostructures," Appl. Phys. Lett. **59**, 2156–2158 (1991).
24. E. C. Young, S. Tixier, and T. Tiedje, "Bismuth surfactant growth of the dilute nitride GaN_xAs_{1-x}," J. Cryst. Growth **279**, 316–320 (2005).
25. H. Ye, Y. Song, Y. Gu, and S. Wang, "Light emission from InGaAs:Bi/GaAs quantum wells at 1.3 μm ," AIP Adv. **2**, 042158 (2012).
26. P. Offermans, P. M. Koenraad, J. H. Wolter, D. Granados, J. M. García, V. M. Fomin, V. N. Gladilin, and J. T. Devreese, "Atomic-scale structure of self-assembled In(Ga)As quantum rings in GaAs," Appl. Phys. Lett. **87**, 131902 (2005).

1. Introduction

The unique properties such as δ -like density of states and good carrier confinement in quantum dots (QDs), in particular III-V compound QDs, have made them very attractive for optoelectronic device applications such as solar cells, lasers and photodetectors [1–3]. InAs/GaAs QD laser is the most studied device due to its low threshold current and very stable temperature dependent bandgap for the fiber optical communication window at 1.3 μm [4]. However, the giant lattice mismatch between GaAs and InAs inevitably builds up excessive internal strain in InAs/GaAs QDs and prevents them from further extending emission wavelength. In addition, QD decomposition upon capping at high growth temperature also incurs decrease in QD height and density [5]. Since Ledentsov *et al.* [6] demonstrated a GaAs-based InAs QDs lasing wavelength record of 1.49 μm at room temperature and 1.51 μm at temperatures above 60 °C in 2003, no one has broken this lasing wavelength record. Although room temperature lasing at 1.55 μm range has been realized using InP-based InAs dots/dash, like in Wang *et al.*'s work [7] who accomplished self-assembled single- and multiple-stack quantum dash lasers on InP (100) substrate with room temperature lasing from 1.60 to 1.66 μm , the InP-based QD technology is significantly less mature than that of GaAs. Due to the difficulty in obtaining high quality distributed Bragg reflectors and less cost-efficient of the substrate in InP-based system, GaAs-based InAs QD system are more advantageous because of the larger substrate size which is more cost-efficient, higher thermal conductivity, larger band offsets and higher refractive index contrast of lattice matched alloys. However, GaAs based InAs QD system also poses a giant challenge for the large lattice mismatch of 7% between GaAs and InAs that will inevitably induce excessive internal strain. For achieving a high performance of InAs/GaAs QD laser, uniform

and dislocation-free QDs with a high density are requisite. Two widely applied methods for maintaining long wavelength emission are using a strain compensation layer underneath InAs QDs and a strain reducing layer above InAs QDs [8–10]. By inserting a tensile strained InGaP compensation layer in the InAs/GaAs QD active region, more than 35% strain reduction was accomplished as verified by high-resolution X-ray diffraction (XRD) [8]. As for the strain reducing layer, InGaAs is usually used and reported to induce a large wavelength red-shift due to the strain relaxation in the apex of InAs QDs along the growth direction [9,10].

Dilute III-V bismide arouses increasing attention recently due to its attractive physical properties such as giant bandgap reduction and spin-orbit splitting energy which can suppress Auger recombination, and temperature insensitive bandgap etc [11–14]. Among all the III-V-Bi alloys, GaAsBi is the most widely studied and reveals a large bandgap reduction of 88 meV/%Bi [11]. In addition, bismuth is reported to act as a surfactant that can influence QDs morphology and also the optical property [15–18]. Both the bandgap reduction effect of GaAsBi and the Bi surfactant effect make GaAsBi very attractive to be employed into the InAs/GaAs QD system and expected to engineer the band structure and strain concomitantly by Bi introduction. Till now, only sporadic studies about Bi influence on QDs morphology and optical properties have been published. Researchers have mainly focused on Bi surfactant effect on QDs: whether the Bi surfactant effect increases or decreases In adatoms diffusion length. Zvonkov et al. [15] and Dasika et al. [16] hold the view that Bi reduces In adatoms diffusion length and prevents QDs coalescence. On the contrary, Okamoto et al. [17] and Fan et al. [18] argue that the Bi surfactant effect enhances In adatoms diffusion length, resulting in large QDs. Except for the surfactant effect, Bi can also be incorporated into GaAs to influence QDs bandgap. Wang et al. [19] used GaAsBi as the strain reducing layer and strain compensation layer for InAs QDs. They observed 23 meV red-shift by embedding InAs QDs between GaAsBi matrix and achieved the longest emission of 1.282 μm at room temperature.

In this work, we systematically investigate the effect of GaAsBi as the lower (strain compensation) and upper (strain reducing) barrier layer on InAs QDs at high (Bi as surfactant) and low (Bi incorporation) growth temperatures, respectively. We demonstrate an improved InAs QDs size distribution upon using Bi as surfactant and a significant redshift by 163 meV with GaAsBi strain reducing layer compared with using GaAs cap layer, leading to emission wavelength of 1.356 μm at 77 K. This provides researchers a new route to overcome the lasing problem of InAs QDs.

2. Experiments

A large number of InAs QDs were grown on semi-insulating GaAs (100) substrates using a solid source DCA P600 molecular beam epitaxy (MBE) system. Growth started with a 200 nm GaAs buffer at 580 °C after the substrate deoxidation process. The growth rate of GaAs and InAs was fixed at 0.4 and 0.1 ML/s, respectively, calibrated by reflection high-energy electron diffraction (RHEED). Growth temperature was kept at 580 and 500 °C for GaAs and all the In-containing layers, respectively, while the Bi-containing layer was grown at 280 and 500 °C for Bi incorporation and surfactant effect investigation, respectively. The temperature below 450 °C was read by a thermocouple while above 450 °C was calibrated by the deoxidation of GaAs at 583 °C. At 280 °C with an As beam equivalent pressure (BEP) = $9.5\text{E-}7$ Torr, we obtained GaAs_{1-x}Bi_x with Bi content of 3% and 5%, respectively, by changing the Bi BEP from $1.9\text{E-}8$ to $3.2\text{E-}8$ Torr. At a high temperature of 500 °C, Bismuth atoms can't be incorporated into GaAs, but acting as a surfactant. Both embedded (in either In_{0.2}Ga_{0.8}As or GaAs_{1-x}Bi_x) and surface QDs were grown on the same sample, separated by a 200 nm thick GaAs, intended for photoluminescence (PL) and atomic layer epitaxy (AFM) measurements, respectively, as sketched in Fig. 1. Three groups of QDs were grown to investigate influence of Bi on InAs QDs. The nominal thickness of all InAs QDs was 2.5 ML, and all the GaAsBi and InGaAs layer for PL were 5 nm. For AFM measurements, surface InAs QDs were capped by 0-32 monolayers (MLs) of GaAs(Bi). Figure 1

schematically illustrates three groups of samples under different growth conditions. Reference samples without Bi introduction were grown under the same growth conditions in each group for comparison.

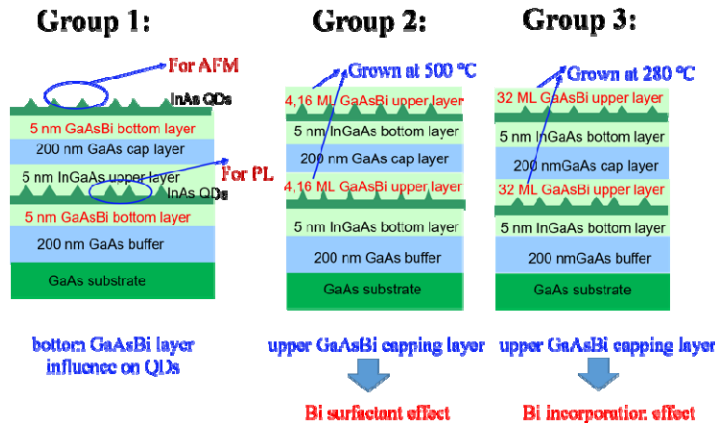


Fig. 1. Illustration of three groups of InAs QDs grown under different conditions.

Bulk GaAsBi materials of 200 nm thick were grown so as to calibrate Bi content. X-Ray Diffraction (XRD) combined with Rutherford backscattering spectrometry (RBS) measurements confirmed 3% and 5% Bi incorporation in GaAsBi grown under the two abovementioned Bi flux, respectively. A Veeco NanoScope IIIa AFM was used to analyze QDs surface morphology. The contact mode was chosen to scan in both 1×1 and $5 \times 5 \mu\text{m}^2$ areas. Photoluminescence spectra was performed by a Fourier Transform Infrared (FTIR) spectrometer (Bruker Vertex 80 v) working under continuous scan mode. Samples were excited by a semiconductor laser ($\lambda = 532 \text{ nm}$) and the diameter of the laser spot was about $200 \mu\text{m}$. Measurement was conducted at 77K cooled down by liquid nitrogen using an InSb detector.

3. Results and discussions

In the following, we will discuss three groups of InAs QDs mediated by Bi in sequence. Each group of InAs QDs was studied by both AFM and PL, respectively. From the AFM results, we explore Bi influence on InAs QDs morphology including QD height, density and distribution, while from the PL measurement Bi influence on QDs peak emission wavelength and intensity is analyzed.

3.1 InAs QDs grown on GaAsBi

In group 1, GaAsBi was grown as the bottom strain compensation barrier layer, prior to InAs QDs growth, as illustrated in Fig. 1. AFM images of surface InAs QDs grown on $\text{GaAs}_{1-x}\text{Bi}_x$ with Bi content of 3% and 5% are shown in Fig. 2(b) and 2(c), respectively, and Bi-free sample in Fig. 2(a) for comparison. By replacing bottom GaAs with $\text{GaAsBi}_{3\%}$, the QD density decreases from $1.26 \times 10^{10} \text{ cm}^{-2}$ to $1.07 \times 10^{10} \text{ cm}^{-2}$ and the average height decreases from 12.0 nm to 10.6 nm as well. In the $\text{GaAsBi}_{5\%}$ sample, the QD density and height further decrease to $1.03 \times 10^{10} \text{ cm}^{-2}$ and 9.2 nm, respectively, as summarized in Fig. 2(d). This can be interpreted that when GaAsBi is grown prior to InAs QDs growth, a high QDs growth temperature of 500°C will cause Bi in the bottom GaAsBi (grown at 280°C) segregating onto surface. Bismuth covering the growing surface lowers surface energy and suppresses In adatoms diffusion. Concomitantly, the critical thickness for transformation from InAs wetting layer to InAs QDs is increased. In a word, Bi delays the onset of InAs QDs formation, resulting in decreased QD density and height.

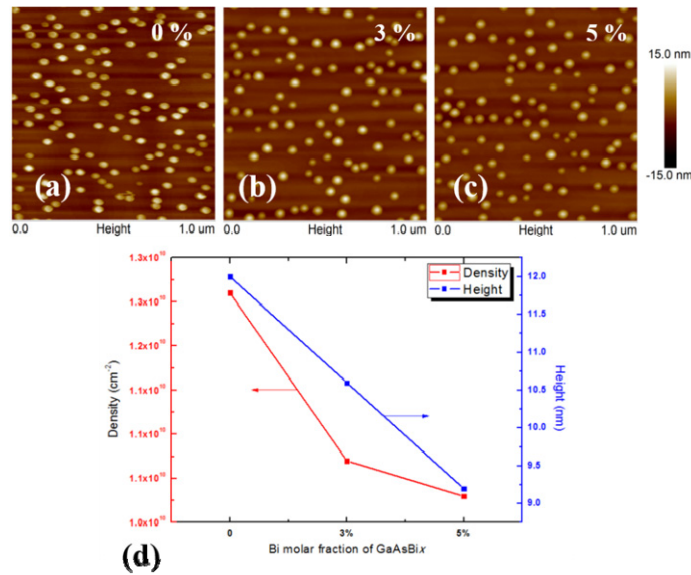


Fig. 2. InAs QDs grown on (a) GaAs; (b) GaAsBi_{3%}; (c) GaAsBi_{5%}, (d) QDs density and height as a function of Bi molar fraction of the bottom GaAs_{1-x}Bi_x.

Figure 3(a) shows PL spectra from InAs QDs grown on GaAsBi and GaAs. The left peaks come from buried InAs QDs and the right wide ones correspond to surface InAs QDs. Each peak consists of two sub-peaks which are preliminarily assigned to coming from the ground and the excited state transitions [20]. Gaussian fitting is employed to extract emission from both the ground and the excited state of QDs, plotted in dashed green (ground state) and red (excited state) lines in Fig. 3(a). For the buried InAs QDs, the ground state emission redshifts from initial 1.006 μm to 1.106 μm and 1.130 μm , respectively, when replacing the underlying GaAs with GaAsBi_{3%} and GaAsBi_{5%}. The significant PL peak wavelength redshift (~ 134 meV) is attributed to the bandgap reduction effect of the GaAsBi barrier. The higher the Bi content in GaAsBi, the narrower the GaAsBi bandgap is. The integrated PL intensity is similar in all the three samples. In addition, energy separation between the excited and the ground state is larger for QDs grown on GaAsBi_{3%} (60 meV) and GaAsBi_{5%} (63 meV) than that on GaAs (45 meV). This increased energy separation in Bi-containing samples in turn indicates the decreased dimensions of QDs size, most likely the QD height, in consistent with the AFM results of surface InAs QDs. Although the repeated surface InAs QDs were grown without an InGaAs capping layer, their surface morphology can still reflect a general feature for the buried InAs QDs. Whereas the PL spectrum evolution for surface InAs QDs was largely different from that of the buried InAs QDs, by increasing Bi concentration in underlying GaAs_{1-x}Bi_x from 0 to 3% and 5%, surface InAs QDs emission initially shows redshift and then blueshift. The bandgap diagram shown in Fig. 3(b) is given to account for this emission difference between the buried and the surface InAs QDs. For the buried InAs QDs, incorporating Bi into GaAs will cause barrier downward, hence redshift the PL. In addition, the higher the Bi content in GaAsBi, the lower the GaAsBi barrier is, and thus the longer the emission wavelength. In spite of a slight decrease in height for the buried InAs QDs as discussed above, we deem that the resulting transition energy change is not so sensitive like that of the surface InAs QDs due to an InGaAs capping layer. As indicated in [21], an InGaAs capping layer is beneficial for preserving QDs size. It is the bandgap reduction effect caused by Bi incorporation contributing most for the giant PL peak energy redshift. Since the height of surface InAs QDs without a capping layer decreases with Bi content in the underneath GaAs_{1-x}Bi_x, a blueshift in transition energy is expected. For QDs

grown on GaAsBi_{3%}, the bandgap reduction effect caused by Bi incorporation outperforms the blueshift caused by the QDs height decrease, thus resulting in an overall redshift. Nevertheless, for GaAsBi_{5%} samples, the two effects will be reverse. In this case, the height decreasing effect of InAs QDs induces a strong blueshift that can't be compensated by the bandgap reduction effect of GaAsBi_{5%}, resulting in an overall blueshift. The narrower PL linewidths of the buried InAs QDs in comparison with those of surface InAs QDs also indicate that an InGaAs capping layer can probably help achieve a uniform QDs size distribution.

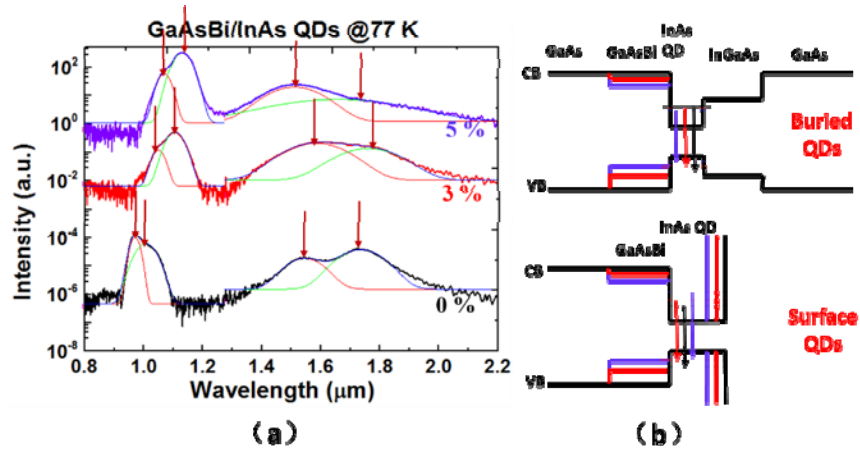


Fig. 3. (a) Photoluminescence spectra measured at 77 K from QDs grown on GaAs, GaAsBi_{3%} and GaAsBi_{5%}, respectively; (b) bandgap diagram of the buried and the surface InAs QDs.

3.2 Bi surfactant effect

In this group, we have grown a set of InAs QD samples capped by 4 and 16 ML GaAs at 500 °C with/without Bi flux. Due to the low solubility of Bi in GaAs at such a high temperature, Bi can hardly be incorporated in GaAs, but act as a surfactant. In addition, an uncapped QD sample was also grown for comparison. AFM results of these InAs QDs are shown in Fig. 4.

The uncapped reference InAs QD sample reveals an approximately equal-weight bimodal distribution in QD height with a total density of $3.6 \times 10^{10} \text{ cm}^{-2}$ and a spread of height in the range of 3-14 nm. The large QDs have an average height of 12 nm while the small ones have an average height of 4.4 nm. The base diameters of the QDs are about 45-50 nm, limited by the AFM tip size. However, the QD height can be measured very accurately up to 0.1 nm. After capping by 4 ML GaAs or GaAs:Bi, the height spread range is similar: 3-12 nm for GaAs and 3-11 nm for GaAs:Bi, but the distribution shape is different. For GaAs capping, it still holds a bimodal centered at 4.0 and 8.4 nm for small and large QDs, respectively, with a total density of $1.88 \times 10^{10} \text{ cm}^{-2}$. This implies that InAs QDs start decomposing upon GaAs capping [5]. When Bi is added during the GaAs capping, the InAs QD distribution becomes uniform with a height centered at 7.6 nm and a total density of $2.0 \times 10^{10} \text{ cm}^{-2}$. Further increasing the cap layer thickness to 16 MLs, volcano-like features appear in both cases and neighboring volcanos start merging together preferentially along the $[1 \bar{1} 0]$ direction. The average height of volcano rims is reduced to 2.4 nm and 1.9 nm for GaAs and GaAs:Bi, respectively, while the total density is about $1.13 \times 10^{10} \text{ cm}^{-2}$ in both cases.

It is well known that InAs QDs will collapse in height and reduce in density upon GaAs capping, the so called QD decomposition process [5]. The driving force for the decomposition process is In segregation due to the fact that InAs has a lower surface energy than that of GaAs. When a GaAs atomic layer is capped on InAs, the capped In atoms have a certain probability to segregate to the growing surface to lower the system energy. This process can

be well simulated by the Muraki's model [22]. For highly lattice mismatched InGaAs grown on GaAs, the initial strain relaxation occurs via formation of InGaAs QDs. For InAs on GaAs, the critical thickness for the onset of QD formation is about 1.7 ML. However, for $\text{In}_{0.5}\text{Ga}_{0.5}\text{As}$, it increases to 4-9 MLs depending on the growth temperature [23]. It means for InAs QDs with a total deposition of less than 2 MLs, capping with 2 ML GaAs would dissolve all existing InAs QDs if the In and Ga intermixing were complete. The growth temperature kinetically limits both lateral (via surface diffusion) and vertical (via surface segregation) In and Ga intermixing. Indium atoms within InAs QDs require external energy to break the In-As bonds and become mobile adatoms on the growing surface. The In surface diffusion is governed not only by the growth temperature on a flat uniform surface but also by surface morphology. The rough surface imposed by large and dense InAs QDs introduces local differences in chemical potentials and thus severely reduces In lateral diffusion length. Likewise, the vertical In segregation is also highly growth temperature dependent.

The 4 ML GaAs equals to a thickness of 1.1 nm. For large InAs QDs capped by 4 ML GaAs, it implies an average height decrease of $12-8.4-1.1 = 2.5$ nm at this particular growth temperature assuming all impinging Ga atoms will not stay on top of the large InAs QDs. For small InAs QDs, the average height of 4 nm is large than $4.4-1.1 = 3.3$ nm, indicating some of the impinging Ga atoms still remain on top of the InAs QDs, or in other word, the QD decomposition is more obvious for large InAs QDs than for small InAs QDs. When Bi is added, small InAs QDs are completely dissolved while large InAs QDs decompose violently with an average height of 7.6 nm, i.e. a decrease of 3.3 nm compared with 2.5 nm without Bi. Bismuth can act as a surfactant at a high temperature by lowering surface energy [24]. It is experimentally shown that with Bi mediation, the critical thickness of InGaAs can be enhanced [25]. Thus capping GaAs:Bi leads to further InAs QD decomposition. As a result, small InAs QDs are completely decomposed, while large InAs QDs also lose a significant amount of constituent In atoms, further reducing the height and becoming uniform. On the other hand, it has been confirmed experimentally by Dasika et al. that adding Bi during InAs QD growth leads to reduction of In surface diffusion length and large QDs coalescence [16]. Therefore, the InAs QD density by capping 4 ML GaAs:Bi is higher than that by capping 4 ML GaAs.

When capping 16 ML (5.5 nm) GaAs, volcano-like features appear in both cases. These features are elongated along the $[1 \ -1 \ 0]$, most likely due to the fast In diffusion compared with the perpendicular $[1 \ 1 \ 0]$ direction [26]. During the QD decomposition, the released In atoms from top of QDs will accumulate at the hillside due to the limited diffusion length, forming plateaus and increasing the base size considerably. Since the top and middle part of an InAs QD are mostly relaxed compare to the QD edges, In atoms are easy to be released forming volcano craters. The crater depth is difficult to measure as the AFM tip can't reach the bottom of the crater. The height of volcano rim for the GaAs:Bi capping is lower than that capped by GaAs. This further supports the surfactant effect of Bi. As the volcano-like features get large, they are difficult to be dissolved. The density will then saturate and the final difference in volcano density is negligible between the two capping.

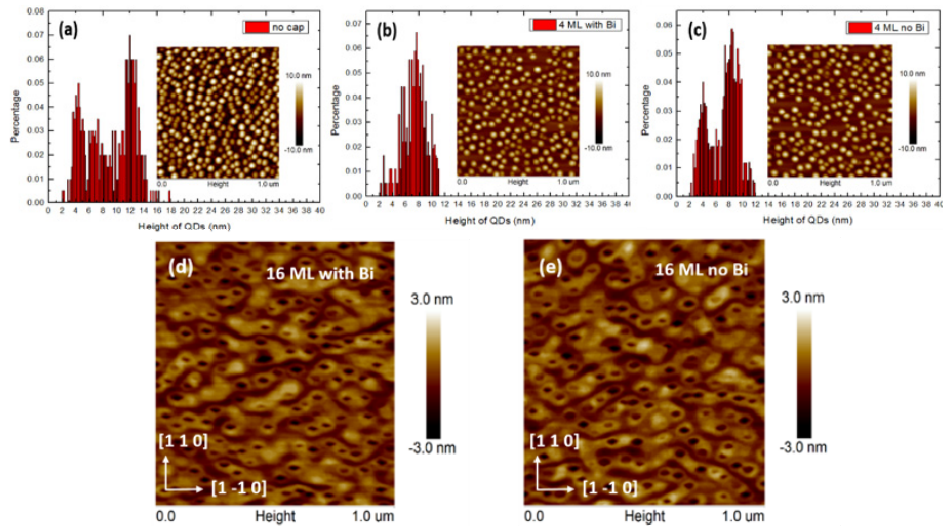


Fig. 4. QDs with different thicknesses of capping layer: (a) no capping; (b) 4 ML GaAs:Bi capping; (c) 4 ML GaAs capping; (d) 16 ML GaAs:Bi capping; and (e) 16 ML GaAs capping.

3.3 Bi incorporation effect

In group 2, during the growth of GaAs capping layer at 500 °C, Bi was supplied to act as a surfactant. In group 3, we reduce the growth temperature of the capping layer to 280 °C to incorporate 3% Bi into 32 ML GaAs intentionally and investigate influence of the cap layer on InAs QDs optical properties. QDs capped with 32 ML (~10 nm) GaAs were also grown for comparison. AFM results of this group sample were omitted here since surface QDs were completely covered in both cases. Figure 5 exhibited a great difference in PL spectral features with different capping layers. The left peaks are emissions from the buried InAs QDs. Although QDs capped by GaAsBi_{3%} exhibited a much weaker PL intensity by a factor of 80 than the GaAs capping, a significant redshift of QDs emission from 1.157 μm to 1.365 μm was observed when replacing GaAs capping layer with GaAsBi_{3%}. Similar result was obtained by Wang et al. who also used a GaAsBi capping on InAs QDs and achieved emission at 1.252 μm at RT [19]. The low growth temperature of 280 °C in our experiment is beneficial for Bi incorporation leading to much long emission wavelength, but inhibits achieving RT emission due to likely non-radiative recombination in GaAsBi. It is concluded that Bi incorporation effect results in an efficient reduction of barrier energy for InAs QDs, inducing a remarkable redshift up to 163 meV. What's more, the linewidth of the PL spectrum from GaAsBi_{3%} capped QDs is significantly narrowed to 50 meV, only half of the value (110 meV) of the Bi-free sample. This is probably due to the Bi surfactant effect that advances an improved QDs size distribution. It is encouraging that by appropriately introducing Bi into InAs QDs growth, Bi surfactant effect combined with its bandgap reduction will help achieve a uniform InAs QDs distribution with long emission wavelength and narrow PL linewidth. The low PL intensity can be improved by post-growth rapid thermal annealing or further optimization of the growth temperature of GaAsBi.

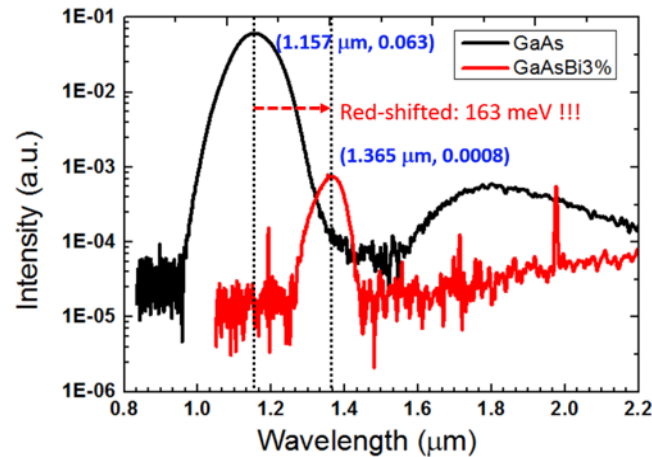


Fig. 5. PL spectra at 77 K of InAs QDs capped with 32 ML GaAsBi (red) and GaAs (black), respectively.

4. Summary

To summarize, we have experimentally fabricated InAs QDs embedded between InGaAs and GaAsBi on GaAs substrates. Using GaAsBi as the bottom strain compensation barrier layer results in decrease in both QDs density and height compared with the Bi-free samples. For GaAsBi capping, at high growth temperature, Bi surfactant effect causes reduction in In adatoms diffusion length, ameliorates QDs density decreasing and improves size distribution. Lowering the growth temperature to 280 °C, the Bi incorporation effect improves QD uniformity and induces a redshift in PL spectrum by 163 meV, leading to an emission wavelength of 1.365 μm at 77 K. Therefore, Bi incorporation and surfactant effect can have a profound effect to engineer InAs QD morphology and optical properties.

Funding

National Natural Science Foundation of China (Grant No. 61404152); National Basic Research Program of China (973 Project) (Grant No. 2014CB643902); Swedish Research Council (VR).

Acknowledgments

We thank Xiren Chen and Jun Shao for providing their FTIR equipment. We also thank professor Shumin Wang for proofreading this manuscript.